Contents lists available at ScienceDirect

Global and Planetary Change

Significant shallow–depth soil warming over Russia during the past 40 years

Liangzhi Chen [a,*], Juha Aalto [a,b], Miska Luoto [a]

[a] *Department of Geosciences and Geography, University of Helsinki, P.O. Box 64, (Gustaf Hällströmin katu 2a), FI-00014, Finland*
[b] *Finnish Meteorological Institute, P.O. Box 503, (Erik Palmenin aukio 1), FI-00560 Helsinki, Finland*

ARTICLE INFO

ABSTRACT

Knowledge of the spatiotemporal dynamics of the soil temperature in cold environment is key to understanding the effects of climate change on land–atmosphere feedback and ecosystem functions. Here, we quantify the recent thermal status and trends in shallow ground using the most up-to-date data set of over 457 sites in Russia. The data set consists of in situ soil temperatures at multiple depths (0.8, 1.6, and 3.2 m) collected from 1975 to 2016. For the region as a whole, significant soil warming occurred over the period. The mean annual soil temperature at depths of 0.8, 1.6, and 3.2 m increased at the same level, at ca 0.30–0.31 °C/decade, whereas the increase in maximum soil temperature ranged from 0.40 °C/decade at 0.8 m to 0.31 °C/decade at 3.2 m. Unlike the maximum soil temperature, the increases in minimum soil temperature did not vary (ca 0.25 °C/decade) with depth. Due to the overall greater increase in maximum soil temperature than minimum soil temperature, the intra-annual variability of soil temperature increased over the decades. Moreover, the soil temperature increased faster in the continuous permafrost area than in the discontinuous permafrost and seasonal frost areas at shallow depths (0.8 and 1.6 m depth), and increased slower at the deeper level (3.2 m). The warming rate of the maximum soil temperature at the shallower depths was less than that at the deeper level over the discontinuous permafrost area but greater over the seasonal frost area. However, the opposite was found regarding the increase in minimum soil temperature. Correlative analyses suggest that the trends in mean and extreme soil temperatures positively relate to the trends in snow cover thickness and duration, which results in the muted response of intra-annual variability of the soil temperature as snow cover changes. This study provides a comprehensive view of the decadal evolutions of the shallow soil temperatures over Russia, revealing that the temporal trends in annual mean and extreme soil temperatures vary with depth and permafrost distribution.

1. Introduction

The soil thermal regime is one of the most fundamental factors influencing terrestrial processes in cold regions (Barry and Gan, 2011; Karjalainen et al., 2019; Streletskiy et al., 2017). Soil temperature is a valuable indicator of climatic change since it integrates multiple processes occurring above and below the land surface. The changing soil temperatures have already had a significant impact on biogeochemical functions, soil hydrology, geomorphologic processes, and infrastructure stability (Cheng and Wu, 2007; Fountain et al., 2012; Grosse et al., 2016; Hjort et al., 2018). Over the past few decades, the frost-affected soil has been at the center of global change research due to its known sensitivity to ongoing climate warming, which is stronger in high latitude areas than the global average (Blunden and Arndt, 2019; Guo and Wang,

2016; Serreze et al., 2009). Permafrost – ground that remains frozen for at least two consecutive years – is mainly distributed across polar and high altitude areas, which are some of the most climate-sensitive places on Earth (Chadburn et al., 2017; Gruber, 2012; Romanovsky et al., 2010; Vieira et al., 2010; Zhao et al., 2010). Compared with research on permafrost areas, the seasonal frost area – where the ground experiences at least 15 days of freezing per year – has received less attention (Tarnocai et al., 2009; Tingjun, 2005).

In permafrost areas over the pan-Arctic, the ground warming near the depth of zero annual amplitude (ZAA) has varied regionally during the past 30 to 40 years, and the warming rate in 2006–2017 was more notable in northern Eurasia (0.33 ± 0.16 °C) than in North America (0.23 ± 0.11 °C) (Biskaborn et al., 2019; Blunden and Arndt, 2019). In particular, the greatest permafrost warming occurred in northeast (0.90

---

* Corresponding author.

E-mail address: liangzhi.chen@helsinki.fi (L. Chen).

°C at Samoylov, 20.75 m) and northwest (0.93 °C at Marre Sale, 10 m) Siberia underlain by continuous permafrost from 2008/2009 to 2016 compared with a global average of 0.29 °C in 2007–2016 (Biskaborn et al., 2019). However, the soil temperature dynamics in shallow depths (0–3 m), especially the extreme soil temperatures, have received less attention. The shallow soil temperatures are more sensitive to seasonality and extremes of air temperature that may largely be filtered out in deep boreholes. The extreme soil temperatures in shallow depths determine the seasonal freeze–thaw depth and thus influence root growth, soil biodiversity, water cycles, vegetation composition, and infrastructure stability (Adriaenssens et al., 2017; Anderson et al., 2019; Porter and Gawith, 1999; Turetsky et al., 2020; Vardon, 2015; Walvoord and Kurylyk, 2016). Furthermore, the soil carbon store down to 3 m depth is nearly triple the size of that stored in the atmosphere and is sensitive to the soil temperature variations, which may be beyond regional consequences but a global concern (Davidson and Janssens, 2006; Fernández-Martínez et al., 2019; Heimann and Reichstein, 2008; Jobbágy and Jackson, 2000).

Due to highly nonlinear heat propagation and inconsistent heat fluxes with depth, soil temperature trends are likely to vary with depth (Baker and Baker, 2002; Phillips, 2020). Meanwhile, the intensity and frequency of extreme weather events are increasing in northern Eurasia, and the response of extreme soil temperatures at multiple depths to climate extremes may be different because of the enhanced thermal filtering ability with depth (Blunden and Arndt, 2019; Groisman et al., 2017). Moreover, frozen soil generally has larger thermal conductivity than unfrozen soil owing to the higher thermal conductivity of ice than water, indicating the necessity of examining the soil temperature changes with the extent of frozen ground (continuous and discontinuous permafrost, seasonal frost) (Côté and Konrad, 2005a, 2005b). Hence, trends in multilayer soil temperatures can be used to validate mechanistic soil temperature models. The knowledge could also advance our understanding of the role of soil temperature in Earth system models as the insufficiency of soil depths in the models has been criticized (Phillips, 2020). In Russia, the shallow-depth soil temperature has been well-documented for decades, especially in the discontinuous permafrost area where knowledge of the ground thermal regime is inadequate because of the sparse borehole monitoring network (Biskaborn et al., 2015; Biskaborn et al., 2019). Therefore, investigations of multiple shallow soil temperature parameters at different depths over a long period (40 years) are indispensable for gaining new insights into the ground thermal status and changes across the region.

Here, we aim to provide a thorough picture of the recent soil temperature variations in Russia. We used a large in situ data set of soil temperature measurements at multiple depths (0.8, 1.6, and 3.2 m) during 1975–2016. We analyzed trends in four soil temperature parameters (mean annual temperature, absolute minimum and maximum temperatures, intra-annual variation) at 457 stations. Finally, we examined the spatial patterns of the trends and contrasted them against current permafrost zonation.

2. Material and methods

2.1. Regional setting

The study region encompasses the land of Russia at latitude >42° N, where the climate varies strongly with latitude and longitude. The mean annual air temperature (MAAT) ranges from −25 to 15 °C, and annual precipitation ranges from ca 200 mm in Siberia to over 2000 mm in Kamchatka and coastal areas of the Black Sea (Groisman et al., 2017; Hijmans et al., 2005). The increase in MAAT over the study region is ca 1.48 °C from the early 1970s to 2010s (Lugina et al., 2006; Park et al., 2014). Taiga dominates the majority of permafrost areas with a tundra belt northward of the tree line (Fig. 1), and the seasonal frost area is covered with a mixture of temperate forest and taiga (Groisman et al., 2017; Tchebakova et al., 2010). In the permafrost area, cryosols and weakly developed soil characterize the zone, and the tundra area is occupied by a diversity of soils in which gleysols prevail with shallow peat coverage (within 30–50 cm). Luvisols with peat coverage dominate the seasonal frost area (Jones et al., 2010).

2.2. Soil temperature data

The daily soil temperature data (from 1975 to 2016) were collected from 457 Russian meteorological stations operated by the All-Russia Research Institute of Hydrometeorological Information – World Data Centre (RIHMI-WDC) (Fig. 1). The soil temperatures at depths ≥0.8 m were measured once a day close to midday under the natural cover of grasses that were cut periodically for station maintenance and snow by a draw-out thermometer with an accuracy of 0.1 °C (Gilichinsky et al.,
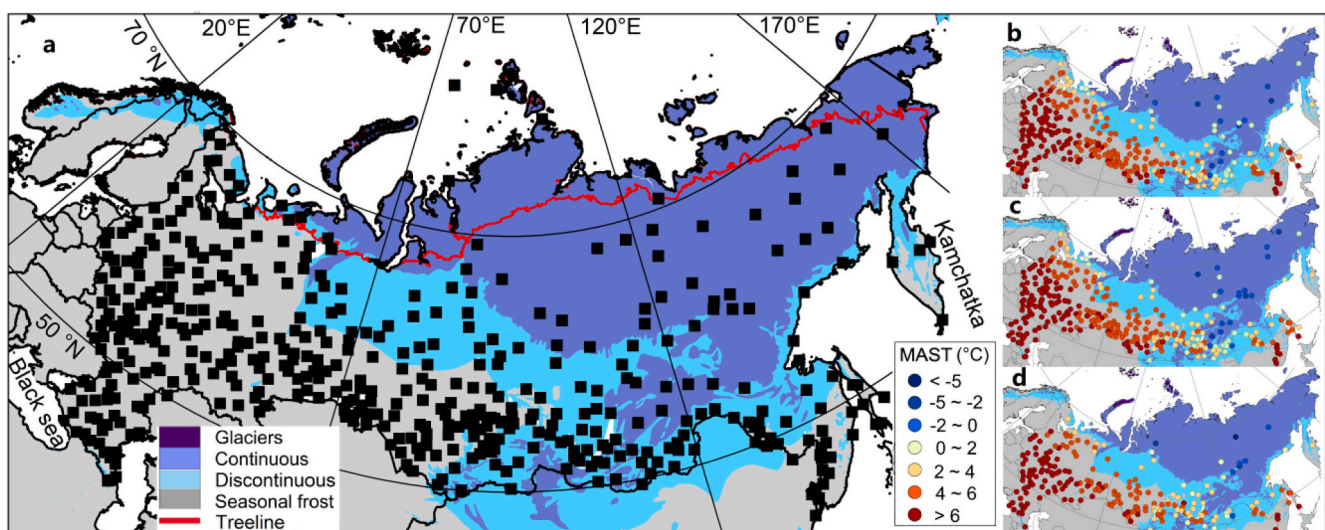

Fig. 1. Soil temperature observation sites. Map a. shows the distribution of observation stations (*n* = 457) across the region. b–d. show the averaged mean annual soil temperatures (MASTs) at depths of 0.8 m (*n* = 315), 1.6 m (*n* = 319), and 3.2 m (*n* = 216), respectively, during 1975–2016. The background map of the permafrost zonation (continuous permafrost area: extent of permafrost ≥90%; discontinuous permafrost area: 0% < extent of permafrost <90%) was obtained from the International Permafrost Association (Brown et al., 1997). The tree line was determined from the Circumpolar Arctic Vegetation Map project (Walker et al., 2005). (For interpretation of the references to colour in this figure legend, the reader is referred to the web version of this article.)

1998). Below a depth of 0.8 m, diurnal temperature variation is mostly damped out (Hinkel, 1997; Hirota et al., 2002; Jacobs et al., 2011). Data gaps are mainly due to the interrupted observations at some sites and depths, but the reasons were not always documented (e.g., harsh weather in winter seasons). Before releasing the data set to the public, RIHMI-WDC undertook multiple quality control checks to maximally exclude suspicious measurements (Sherstiukov, 2012). First, visual inspection of the distributions and neighboring values for the raw data were used to reveal apparent errors (e.g., unphysical values or reversed signs). Second, outlier detection using 4σ (standard deviation, SD) was applied to ensure that the data were within a reasonable range. Finally, the connectedness of neighboring values was evaluated to reveal irregular errors in analyzing successive days (see Text S1). Consequently, none of the data were artificially adjusted but they were flagged for quality levels. Only data flagged as "reliable" were analyzed in this study (see Text S2). The observational periods and depths are inconsistent at the sites. Therefore, we used the data collected from depths of 0.8, 1.6, and 3.2 m because of satisfactory spatiotemporal coverage.

2.3. Soil temperature parameters and temporal trends

Four parameters were computed from the daily soil temperature measurements: annual mean temperature (MAST, °C), annual maximum temperature (T_{max}, °C), annual minimum temperature (T_{min}, °C), and intra-annual variation ($T_{range} = T_{max} - T_{min}$, °C). The parameters were calculated for all sites in each calendar year from 1975 to 2016, during which T_{min} was observed from January to July for most of the years (more than 95–99%) depending on depth (Table S1). On average, less than 5% (no more than two days) of data per month are missing (Table S2) and 362 days (minimum 300 days) of data are available in a year at three depths (Table S3).

The temporal trends in parameters were derived from the slopes of linear least squares regressions during a minimum of 30 years from 1975 to 2016. Consequently, regional soil temperature evolution was assessed by integrating results over 457 sites. The variations in soil temperature trends were visualized by kernel density estimation and box-and-whisker plots based on the packages of sm and ggplot2, respectively, in R (Bowman and Azzalini, 1997; R Core Team, 2017; Wickham, 2016). Moreover, we used the Wilcoxon method (Gehan, 1965) to test the statistical significance of the trends in soil temperature against the null (0 °C/decade).

2.4. Air temperature and snow cover characteristics

We used air temperature (2 m above the land surface) and snow cover depth data to examine the influence of snow cover on soil temperature and the temperature offset between air and soil. Archived daily mean air temperature was the average of three-hourly measurements for each calendar day with an accuracy of 0.1 °C, and daily snow depth was measured once per day with an accuracy of 0.1 cm (Bulygina and Razuvaev, 2012). The MAAT and minimum annual air temperature were computed by daily measurements at the sites where the soil temperature data were available during 1975–2016. Consequently, the annual offset ($\Delta T_{0.8}$) is defined as the magnitude of the difference between mean annual soil temperature ($MAST_{0.8}$) and MAAT ($\Delta T_{0.8} = MAST_{0.8} -$ MAAT, °C). Similarly, the annual sum of snow depth (SSD, cm) and snow cover duration (SCD, days) were derived from the daily snow cover depth. Moreover, the trends in SCD and SSD were calculated following the same criteria for computing the trends in soil temperature.

3. Results

3.1. Trends in soil temperature from 1975 to 2016

It is found that MAST increased at 279, 286, and 197 sites, while it decreased at 4, 2, and 2 sites, and remained stable (within measurement accuracy) at 32, 31, and 17 sites at depths of 0.8, 1.6, and 3.2 m, respectively (Fig. 2a). The greatest warming of MAST at shallow depths (0.8 and 1.6 m) is 1.09 ± 0.20 °C/decade (mean $\pm$ SD, $P < 0.01$) at a site located in the northern Siberian permafrost area. At a deeper level (3.2 m), the greatest warming in MAST occurred in central Siberia at 0.89 ± 0.12 °C/decade ($P < 0.01$). However, a few sites that had decreased MAST are mainly located in the permafrost area. Trends in MAST from -0.11 to -0.21 °C/decade were observed at four sites at 0.8 m. For the depths of 1.6 and 3.2 m, MAST of the two sites located in the continuous permafrost area decreased by 0.15 ± 0.09 ($P > 0.05$) and 0.11 ± 0.05 °C/decade ($P > 0.05$), respectively, and a decrease in MAST at 3.2 m of 0.36 ± 0.06 °C/decade ($P < 0.05$) occurred at a seasonal frost site.

In the region as a whole, soil temperature of shallow ground significantly increased over the past four decades (Fig. 3). For example, MAST on average increased by ca 0.30 °C/decade at multiple depths at over 80% of the significant sites ($P < 0.05$); in particular, at 3.2 m, 89% of the sites had a significant trend in MAST (Table 1). The warming rate of T_{max} was greater than that of T_{min}, which led to an increase in T_{range} across the region. The trend in T_{max} at the shallow depth (0.40 °C/decade at 0.8 m) was greater than at the deeper level (0.33 °C/decade at 3.2 m), whereas the trend in T_{min} remained relatively stable at ca 0.25 °C/decade at all depths. T_{range} significantly increased (ranging from 0.08 to 0.15 °C/decade with depth) over the period, with less than 50% significant sites. Notably, the proportion of sites associated with a significant trend in T_{min} at 3.2 m (80%) is much higher than that at other depths (less than 60%), which may partially be attributed to the different levels of latent heat effects from the freeze–thaw cycles that occurred at over half of the insignificant sites at 0.8 m but at only 6% at 3.2 m (Table 1). The filtering effect of depth also contributes to the magnitude of the proportion as a significant trend may be more detectable at a deeper level where the soil temperature is less variable than at the shallow depth (Qian et al., 2011).

The trends in soil temperature varied regionally with the extent of frozen ground (Fig. 4). At depths of 0.8 and 1.6 m, the increase in MAST in the continuous permafrost area was the fastest, followed by the soil warming rates in the seasonal frost and discontinuous permafrost areas. However, at 3.2 m, the warming of the soil in the continuous permafrost area (0.26 °C/decade) was ca 20% less than that in the discontinuous permafrost area (0.31 °C/decade). This could partially be attributed to the different latent heat effect levels, which are primarily controlled by the soil moisture and active layer thickness. In the discontinuous permafrost area, the warming of the soil is likely to be decelerated under the more significant effects of freeze–thaw cycles and latent heat than in the continuous permafrost area. Besides, the warming rate of the soil temperature in the seasonal frost area is less compared with that observed in the continuous permafrost area but larger than in the discontinuous permafrost area. The increase in T_{max} in the discontinuous permafrost area was greater at 3.2 m compared with at the shallow depth, but the opposite was the case for T_{min}. However, over the seasonal frost area, the trend in T_{max} diminished from 0.40 to 0.32 °C/decade with depth, while the increase in T_{min} ranged from 0.19 to 0.25 °C/decade. The increase in T_{min} over the seasonal frost area (0.19 °C/decade) was much less than in the permafrost area (0.30–0.56 °C/decade) at 0.8 and 1.6 m, indicating more significant latent heat effects at the shallower depths. T_{range} significantly increased by 0.24 °C/decade at 0.8 m and diminished to 0.07 °C/decade at 3.2 m in the seasonal frost area, whereas the trend was not clear in the permafrost area.

3.2. Impact of snow cover characteristics on soil temperature

It is found that MAST was, in general, higher than MAAT, accounting for 0.64 of MAAT at all sites (Fig. 5a). Meanwhile, the sites with smaller SSD and SCD (lighter dots) are closer to the 1:1 line, indicating the role of snow cover in offsetting MAST against MAAT. SSD and SCD were both positively related to $\Delta T_{0.8}$ (Fig. 5b and c), whereas the relations between $\Delta T_{0.8}$ and two snow cover parameters are different, with $\Delta T_{0.8}$–SSD
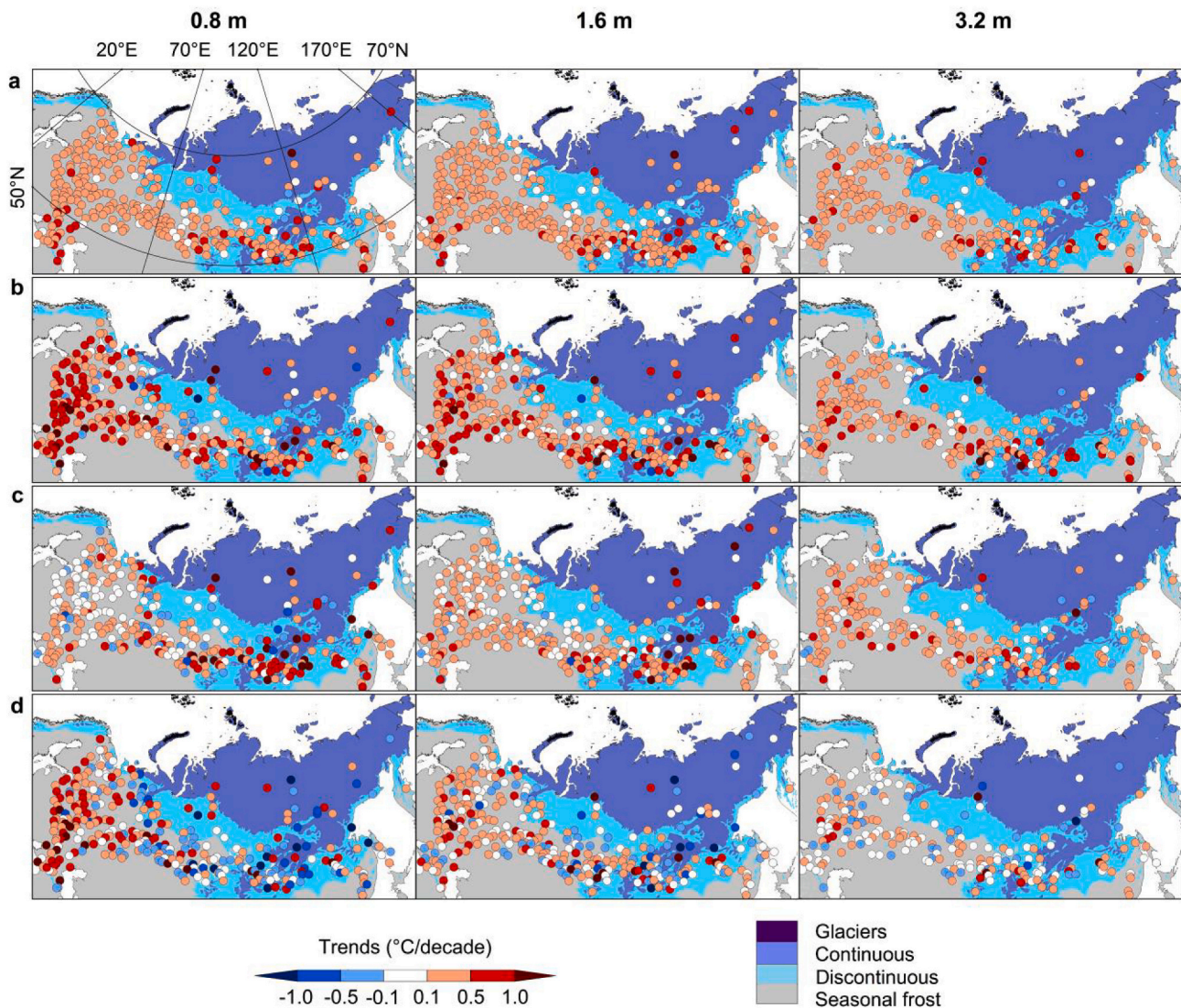
Fig. 2. Spatial distribution of the trends in MAST (a), T_{max} (b), T_{min} (c), and T_{range} (d) from 1975 to 2016 at multiple depths. There are 315, 319, and 216 sites at depths of 0.8, 1.6, and 3.2 m, respectively.

relations being more linear than $\Delta T_{0.8}$–SCD relations. Moreover, SCD shows a higher R^2 (0.49) than SSD (0.40) in the linear relationship with $\Delta T_{0.8}$.

In general, there were significant positive relations between the trends in snow cover and soil temperatures, with the exception of the negative relations between the trends in T_{range} and snow cover (Fig. 6). Notably, the five cooling sites were all accompanied by the decreased SSD and SCD during the period (Fig. 6a and b). Relations between the trends in temperature (MAST, T_{min}) and SSD are stronger than the trends in SCD with a higher coefficient of determination (R^2), indicating that the changes in snow cover depth may be more influential in affecting the soil temperature than the SCD. However, the relation between the trends in T_{range} and SCD is slightly stronger than between T_{range} and SSD.

The minimum soil temperature in winter can be affected by the freezing latent heat. At Yakutsk, the freezing zero-curtain of the soil temperature at depths of 0.8 and 1.6 m last 46 and 96 days in 1995, respectively, which are longer than observed in 1996 (32 and 76 days) (Fig. 7). It is noted that the longer zero-curtain period is associated with deeper snow cover. For example, the mean snow cover depth in 1995 (11.3 cm) was over three times that in 1996 (3.7 cm) during the zero-curtain period at a depth of 0.8 m. The long-curtain period decelerated the cooling of the soil after the air temperature went below 0 °C.

Consequently, the minimum soil temperature in 1995 was 2.5 °C higher than that in 1996 despite a 2.3 °C lower minimum air temperature in 1995.

4. Discussion

The annual mean and extreme soil temperatures of shallow ground significantly increased from 1975 to 2016 in Russia. The majority of the sites had warming trends, and a few sites mainly located in the permafrost areas remained thermally stable and even cooled during the period. The soil warming in the continuous permafrost area was faster than that in the discontinuous permafrost and seasonal frost areas at 0.8 m and 1.6 m, and was slower at 3.2 m (Fig. 4). Moreover, the annual maximum soil temperature increased faster than the minimum soil temperature, which led to increased intra-annual variability of soil temperature (Fig. 3). The study provides an unprecedentedly detailed picture of soil temperature evolution over the past four decades in Russia by quantifying the trends in the multilayer soil temperature parameters at 457 sites.

It is notable that variations in the trends of MAST and T_{min} over the discontinuous permafrost area were smaller than those in the continuous permafrost in the shallow depth but at a similar level at 3.2 m. This is
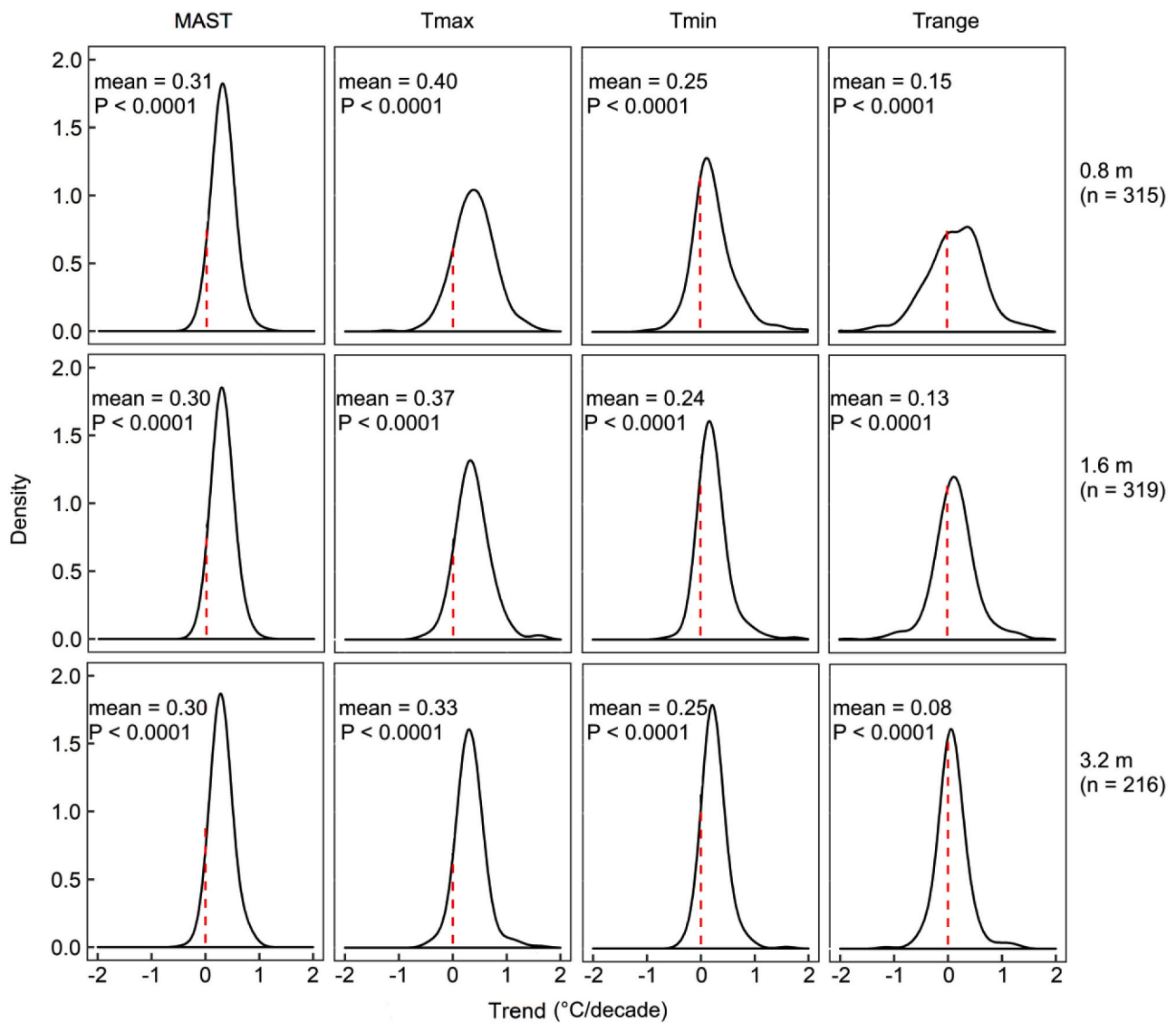
Fig. 3. Density distribution of the trends in soil temperature from 1975 to 2016. The kernel-smoothed distributions (bandwidth = 0.15) represent estimated soil temperature trends in the four parameters (MAST, T_{max}, T_{min}, T_{range}) at multiple depths. The significance of the distributions was tested against the null (0 °C/decade, indicated by red dashed line) based on the Wilcoxon method. (For interpretation of the references to colour in this figure legend, the reader is referred to the web version of this article.)

Table 1
Summary of linear regression analyses for the four soil temperature parameters with depth from 1975 to 2016.

Parameter	Depth (m)	Mean years[a]	Mean changes[b] (S.D.) (°C/decade)	N_{sites}	significant sites (%) ($P < 0.05$)[c]	insignificant sites (freeze - thaw affected)[d]
MAST	0.8	35.5	0.31 (0.18)	315	81	48 (76%)
	1.6	35.6	0.30 (0.17)	319	83	19 (34%)
	3.2	35.3	0.30 (0.18)	216	89	3 (11%)
T_{max}	0.8	35.5	0.40 (0.39)	315	63	92 (77%)
	1.6	35.6	0.37 (0.33)	319	70	31 (32%)
	3.2	35.3	0.33 (0.26)	216	81	3 (6%)
T_{min}	0.8	35.5	0.25 (0.41)	315	39	112 (58%)
	1.6	35.6	0.24 (0.31)	319	56	44 (30%)
	3.2	35.3	0.25 (0.21)	216	80	3 (6%)
T_{range}	0.8	35.5	0.15 (0.59)	315	46	124 (72%)
	1.6	35.6	0.13 (0.44)	319	44	51 (28%)
	3.2	35.3	0.08 (0.28)	216	43	4 (3%)

[a] Mean number of years used for computing the trends at all sites.

[b] SD = standard deviation.

[c] *P* value was derived from the linear regression for each site.

[d] A site was affected by the freeze–thaw cycles if the averaged maximum and minimum soil temperatures during 1975–2016 were above and below 0 °C, respectively.
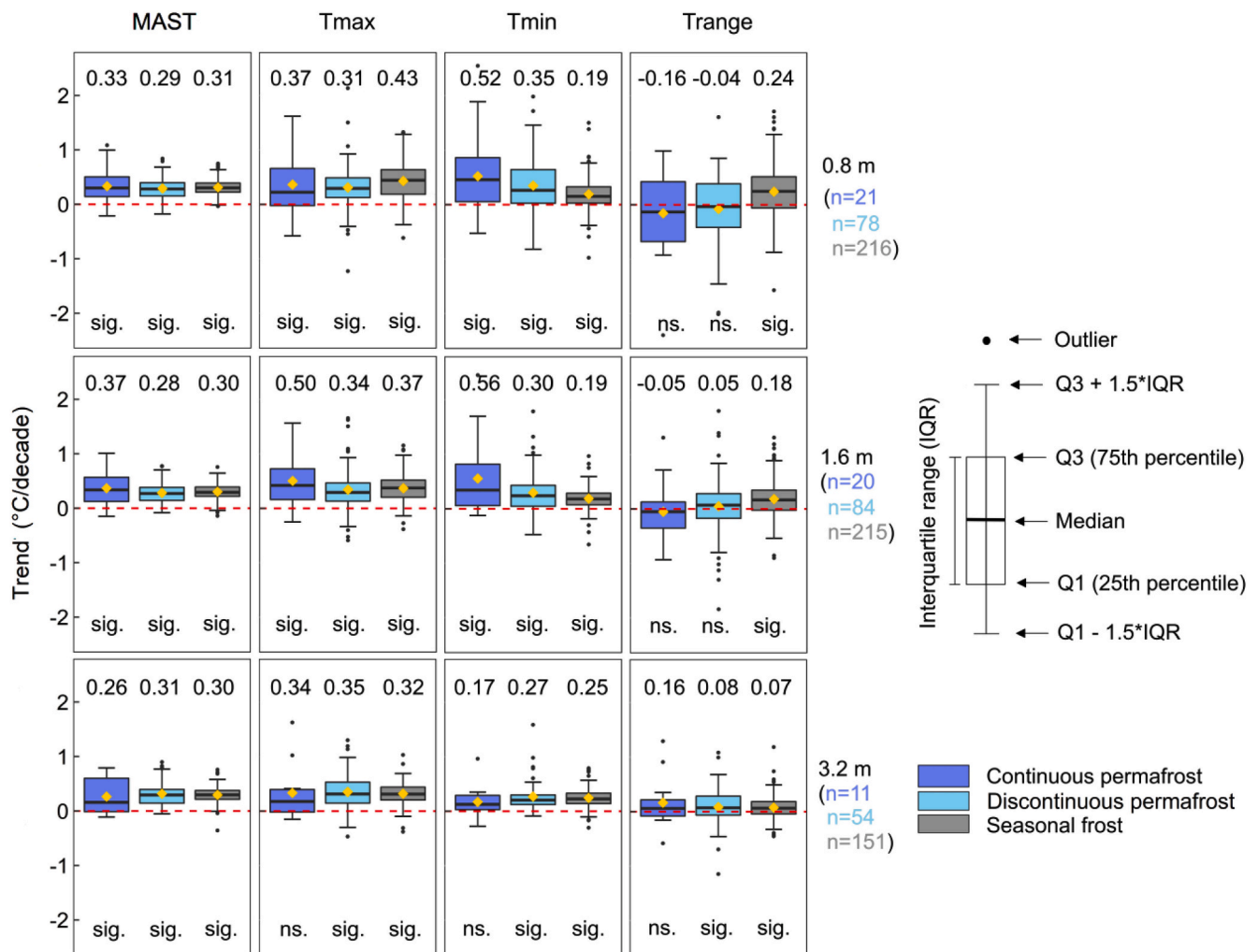
Fig. 4. Box plots depict the distribution of the trends in soil temperature with depth and permafrost distribution from 1975 to 2016. The significance of each distribution relative to 0 °C/decade (red dashed line) was tested by the Wilcoxon method and is indicated by either sig. (significant, $P \leq 0.05$) or ns. (not significant, $P > 0.05$). The mean of each distribution are marked with yellow diamonds and reported at the top. (For interpretation of the references to colour in this figure legend, the reader is referred to the web version of this article.)

presumably because the soil in the discontinuous permafrost area involves a more pronounced ice–water phase change process due to the thicker active layer than in the continuous permafrost area. Thus, more latent heat is needed to thaw the active layer in the discontinuous permafrost area, which is likely to resist the increase in MAST (James et al., 2013; Romanovsky et al., 2010; Zhang et al., 2001). At depths of 0.8 and 1.6 m, the increase in T_{min} over the seasonal frost area was slower than that of T_{max}, whereas in the continuous permafrost area, T_{min} increased faster than T_{max}, which might advance talik development as the soil at these depths cannot refreeze and will remain thawed in a warm climate (Jafarov et al., 2018; Jorgenson et al., 2010). Of note, in the continuous permafrost area, the warming of MAST at 1.6 m (0.37 °C/ decade) was greater than that at 0.8 m (0.33 °C/decade), whereas the warming rates were similar in the discontinuous permafrost and seasonal frost areas. It can be interpreted that warming in the upper soil could take some time to reach deeper in the continuous permafrost area, but once warmed, the deeper layer remains warm later in the year (Qian et al., 2011). Consequently, the heat trapped in the deep levels can trigger permafrost degradation, enhancing organic matter decomposition in permafrost and thereby positively contributing to climate warming (MacDougall et al., 2012; Schuur et al., 2013; Schuur et al., 2015). The magnitude of T_{range} is dependent on the ground thermal properties and land cover conditions (Christiansen et al., 2010;

Romanovsky et al., 2010; Smith et al., 2010). Our results suggest a negative relation between trends in T_{range} and snow cover characteristics, which may relate to a positive relationship between the trends in snow cover and T_{min} (Fig. 6).

Air temperature is a major control of soil temperature (Grosse et al., 2016; Park et al., 2014; Smith et al., 2010). In the study region, the increase in MAAT was ca 0.37 °C/decade during 1975–2011. However, the air temperature changes alone cannot account for the increase in soil temperature (MAST ca 0.30 °C/decade), indicating that the temperature in shallow ground increased less than the air temperature in Russia during the period. The response of soil temperature to the changes in snow cover conditions is significant (Fig. 6). The trends in soil temperature positively related to snow cover trends and the sites with decreased MAST are consistently associated with decreases in snow cover depth and duration (Fig. 6). Similarly, in interior Alaska, the decrease in permafrost temperature measured near the depth of ZAA during 2007–2013 was attributed to the relatively shallow snow cover during the period (AMAP, 2017; Romanovsky et al., 2015).

The role of snow cover in mitigating soil temperature has been widely examined (Lawrence and Slater, 2010; Morse et al., 2012; Romanovsky et al., 2007; Tingjun, 2005; Zhang et al., 2018). The snow cover generally offset the soil and air temperatures by insulating ground from the cold in winter, whereas a late snow cover onset in autumn or
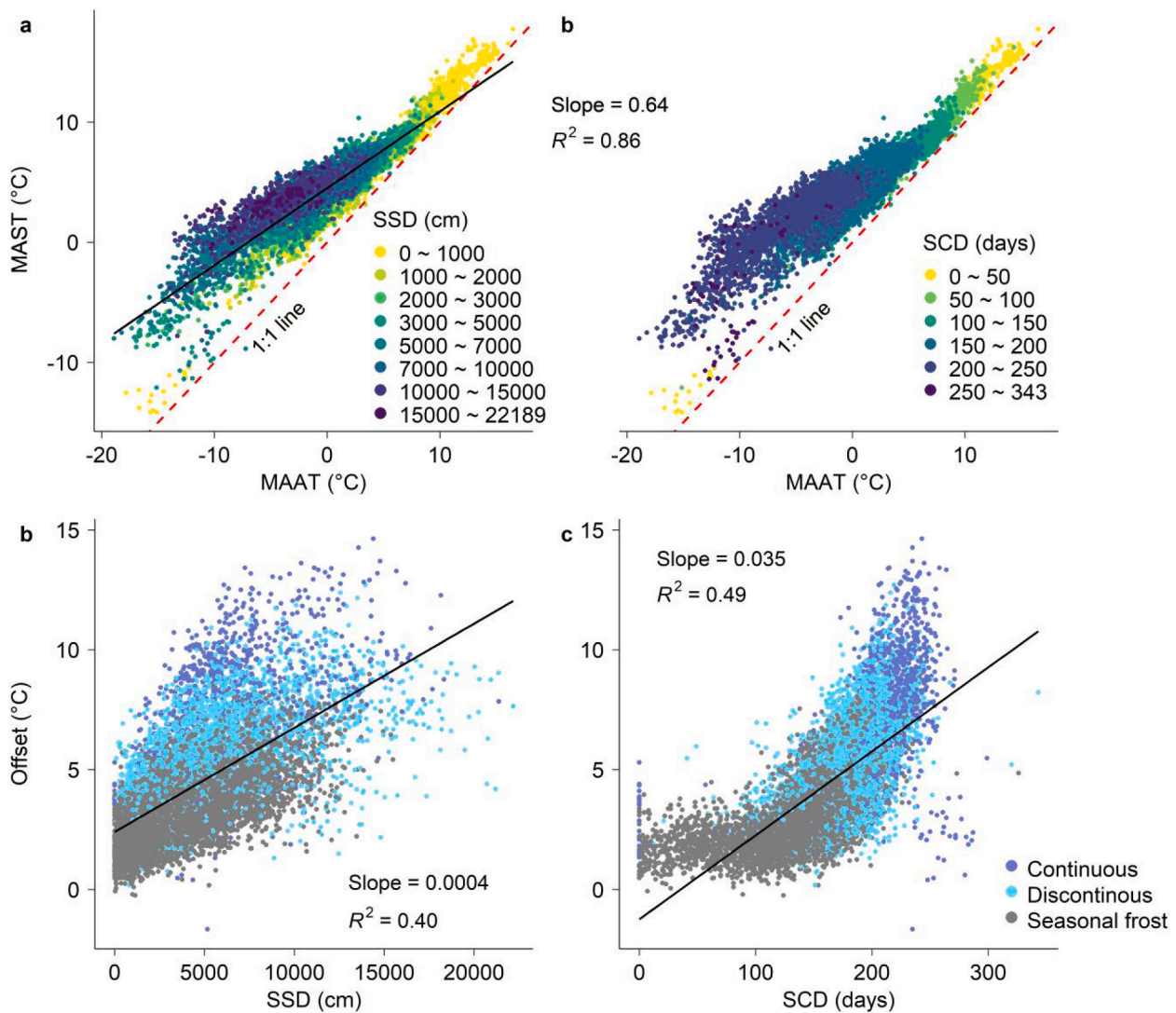
Fig. 5. a. Relationships between the mean annual soil temperature (MAST, 0.8 m) and air temperature (MAAT). In total, 9722 annual values at 269 sites during 1975–2016 are scattered with colour representing the annual sum of snow depth (SSD, left) and snow cover duration (SCD, right). b, c. Relationships between the annual offset ($\Delta T_{0.8}$) and SSD (b) and SCD (c) with permafrost distribution.

winter with late snowmelt in spring may have an overall cooling effect on the annual soil temperature (Bonnaventure and Lewkowicz, 2012; Euskirchen et al., 2007; Morse et al., 2012; Palmer et al., 2012; Smith et al., 2016). The strength of snow cover effects on MAST–MAAT coupling is not only dependent on the air temperature, active layer thickness but also on substrate material and soil moisture content (Iijima et al., 2010; Throop et al., 2012). For instance, it is noticeable that some sites have close relationships between MAST and MAAT despite the massive and long snow cover during winter, which can be attributed to the limited latent heat effect due to the local substrate and soil moisture conditions (Fig. 5a and b). Throop et al. (2012) conclude that, at the Alert site, which was built on bedrock in far northern Canada, a high coupling (0.80–0.96) between MAGT (mean annual ground temperature measured at 15.4–16.0 m) and MAAT is due to the ice-poor overburden layer above the bedrock, which significantly reduces the latent heat effect and thus allows rapid refreezing of the active layer and decrease in ground temperature, consequently, improving the coupling of MAGT–MAAT. However, the sites underlain by unconsolidated sediments are more strongly affected by latent heat owing to higher soil water content and larger porosity.

Moreover, the influence of snow cover on soil temperature aggregates the effects of snow cover thickness, duration, and timing. Smith et al. (2012) highlight that soil temperature trends at the sites with greater snow cover show a muted response to air temperature trends, especially if largely due to winter and autumn air temperature change. However, if snow cover is changing over time, this can either enhance or counteract the effect of changing air temperature on soil temperature trends (AMAP, 2017; Taylor et al., 2006). For instance, permafrost warming during 1970–1990 in northern Russia was attributed to enhanced snow accumulation rather than increased air temperature (Pavlov, 1994; Stieglitz et al., 2003). In the Canadian Arctic, warming of the permafrost from 1950 to 1975 at Alert was dominated by increased snow cover despite a decreased MAAT (Taylor et al., 2006).

The impact of other factors on soil temperature can be more complicated than that of air temperature. In the seasonal frost area, an increase in snowfall in early winter has a strong positive impact on the soil thermal regime, whereas late snowfall may have a negative impact due to the high albedo and consumption of latent heat during snowmelt (Zhang et al., 2001). Moreover, the ratios of rainfall to snowfall and evapotranspiration, even the amount of total precipitation, closely relate to the variations of air temperature (Bintanja and Andry, 2017). As such, changing precipitation regime modifies soil moisture content and thermal conductivity, further affecting the soil temperature (Westermann et al., 2011). For instance, warming of the ground in the central Lena
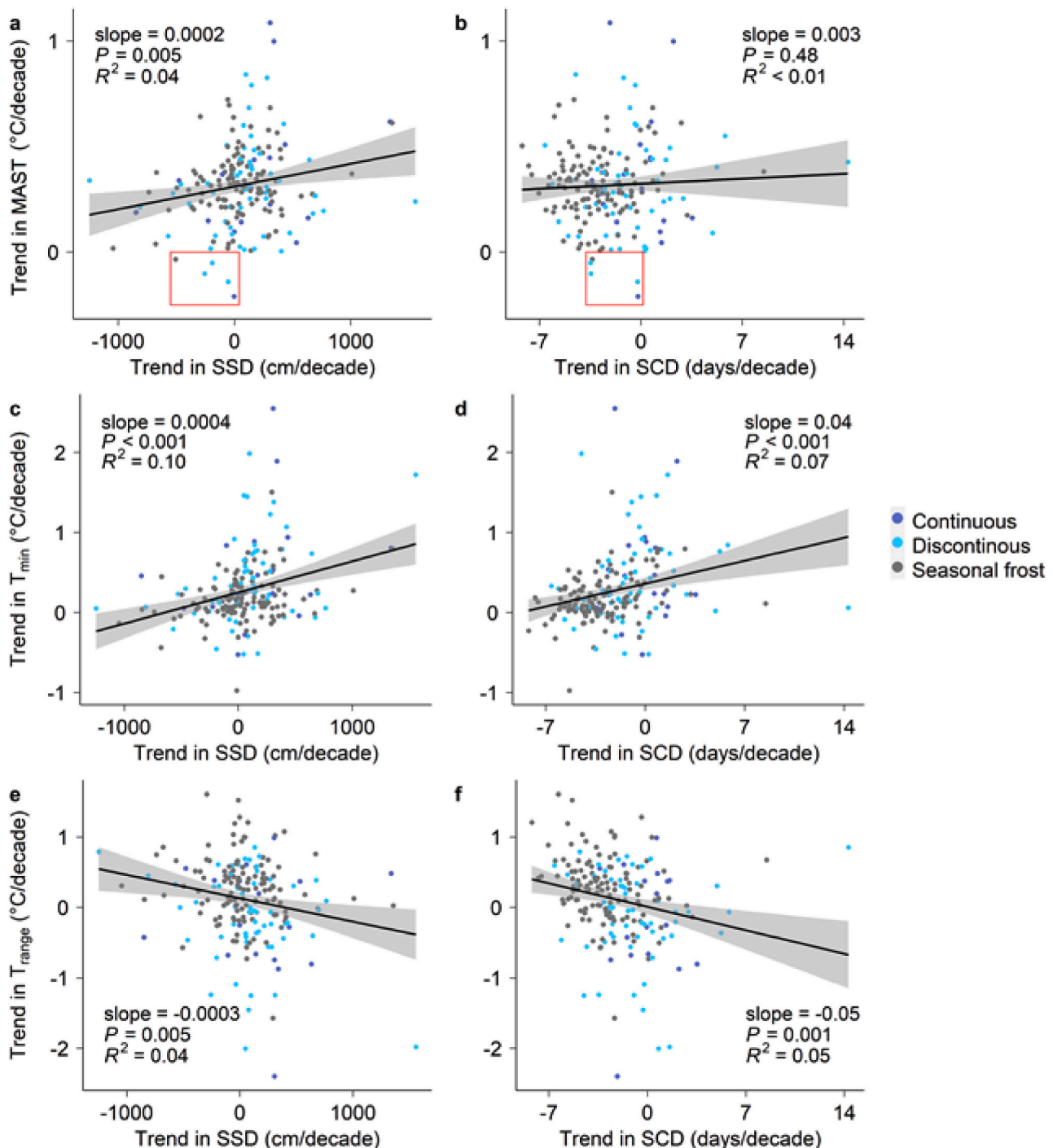
Fig. 6. Linear relationships between the trends in snow cover characteristics (sum of snow depth [SSD] and snow cover duration [SCD]) and MAST (a, b), T_{min} (c, d), and T_{range} (e, f) at a depth of 0.8 m. There are 196 paired sites, of which 19, 56, and 121 are located in the continuous permafrost, discontinuous permafrost, and seasonal frost areas, respectively. Red rectangles in a and b indicate the sites that had decreased MAST during the period. (For interpretation of the references to colour in this figure legend, the reader is referred to the web version of this article.)

River basin in eastern Siberia occurred in response to an increase in rainfall during the pre-winter periods between 2004 and 2007 (Iijima et al., 2010). Moreover, local and regional scale studies have highlighted the importance of vegetation in affecting soil temperature (Bonan, 2015; Karjalainen et al., 2019). An experimental study at high Siberia suggested that removal of shrubs significantly alters ground heat flux, which thickens the active layer of the permafrost and increases summer soil temperature (Blok et al., 2010; Nauta et al., 2015). Thus, regular cuts of grasses at stations in summer may act as a non-climatic

contributor to soil warming (Gilichinsky et al., 1998). This can be further complex considering the interactions between air temperature and vegetation dynamics as it has been demonstrated that increase in air temperature sometimes causes vegetation changes that can offset the warming of soil against air (Bonfils et al., 2012; Walker et al., 2003; Yi et al., 2007).
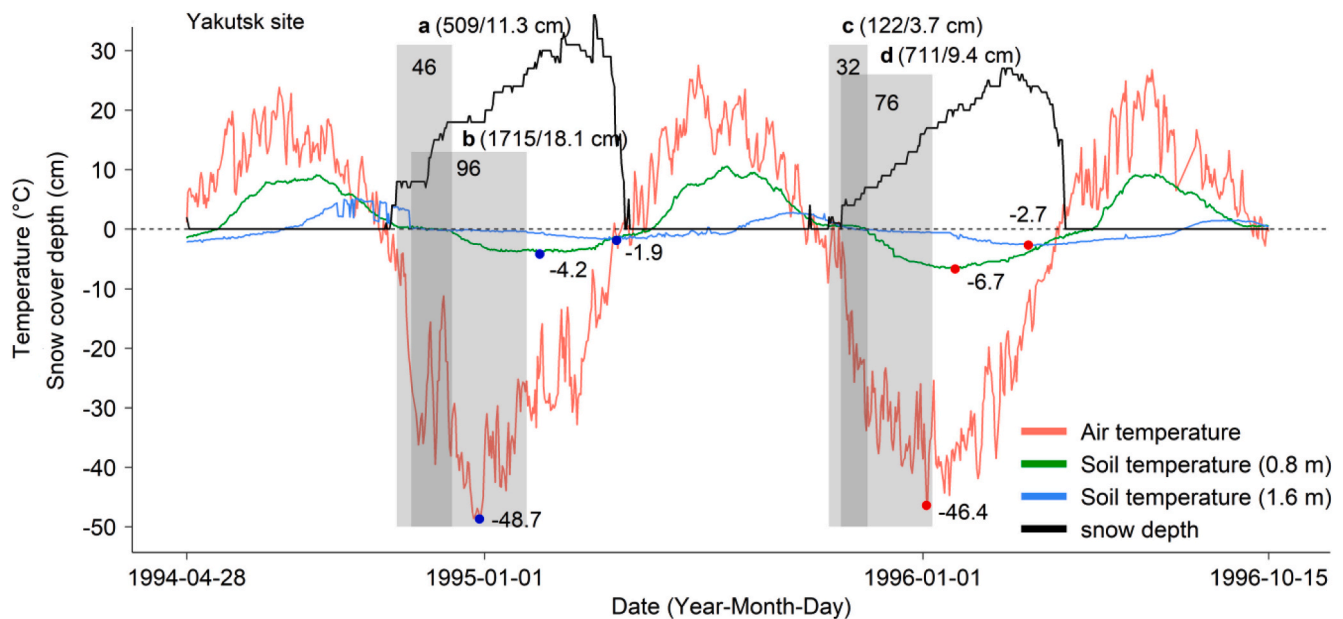
Fig. 7. Influence of the freezing zero-curtain length on soil temperature. Yakutsk (62.017° N, 129.717° E, 98 m a.s.l.) is located in the discontinuous permafrost area. High (a, c) and low (b, d) shades cover the zero-curtain period (temperatures remain within ±0.4 °C) at depths of 0.8 and 1.6 m, respectively, during two winter seasons. The numbers in brackets represent the snow cover conditions in the zero-curtain period (sum of snow depth/mean snow depth, cm). The numbers in shades indicate the length of the zero-curtain period. The blue and red dots mark the days on which the minimum temperatures were observed. (For interpretation of the references to colour in this figure legend, the reader is referred to the web version of this article.)

5. Conclusions

By quantifying the trends in multiple soil temperature parameters over the areas with a different extent of frozen ground, we found significant shallow ground warming over Russia from 1975 to 2016. Beyond the MAST, the increases in extreme and intra-annual variability of soil temperature varied with depth and permafrost distribution. This highlights the importance of discriminating the areas by the extent of frozen ground in future studies, when soil temperature, especially extreme temperature, is involved at a regional scale. The results provide a set of benchmark data for regional soil temperature models and may also have broader implications in urban development, agriculture, and infrastructure over the region in the future with denser human activities through the region (Groisman et al., 2017; Hjort et al., 2018).

The current soil temperature monitoring network in the region is sparse, especially over the northern Siberia permafrost area, limiting the spatial resolution of the analyses and bringing some uncertainties. Despite a data deficit of less than five days a year, an average 36-year time series analysis during 1975–2016 is likely to emerge as a basis for the results. Considering ongoing climate change and its consequences, the thermal interactions near the land–atmosphere interface keep changing (AMAP, 2017; Biskaborn et al., 2019; Blunden and Arndt, 2019; Hjort et al., 2018). Thus, continuous and enhanced monitoring of soil temperatures is required.

Appendix A. Supplementary data

Supplementary data to this article can be found online at https://doi.org/10.1016/j.gloplacha.2020.103394.

References

Adriaenssens, E.M., Kramer, R., Van Goethem, M.W., Makhalanyane, T.P., Hogg, I., Cowan, D.A., 2017. Environmental drivers of viral community composition in Antarctic soils identified by viromics. Microbiome 5 (1), 83. https://doi.org/10.1186/s40168-017-0301-7.

AMAP, 2017. Snow, Water, Ice and Permafrost in the Arctic (SWIPA) 2017. Arctic Monitoring and Assessment Programme(AMAP).

Anderson, J.E., Douglas, T.A., Barbato, R.A., Saari, S., Edwards, J.D., Jones, R.M., 2019. Linking vegetation cover and seasonal thaw depths in interior Alaska permafrost terrains using remote sensing. Remote Sens. Environ. 233, 111363. https://doi.org/10.1016/j.rse.2019.111363.

Baker, J.M., Baker, D.G., 2002. Long-term ground heat flux and heat storage at a mid-latitude site. Clim. Chang. 54 (3), 295–303. https://doi.org/10.1023/A:1016144718218.

Barry, R., Gan, T.Y., 2011, August. The Global Cryosphere: Past, Present and Future. Cambridge Core. https://doi.org/10.1017/CBO9780511977947.

Bintanja, R., Andry, O., 2017. Towards a rain-dominated Arctic. Nat. Clim. Chang. 7 (4), 263–267. https://doi.org/10.1038/nclimate3240.

Biskaborn, B.K., Lanckman, J.-P., Lantuit, H., Elger, K., Streletskiy, D.A., Cable, W.L., Romanovsky, V.E., 2015. The new database of the Global Terrestrial Network for Permafrost (GTN-P). Earth Syst. Sci. Data 7 (2), 245–259. https://doi.org/10.5194/essd-7-245-2015.

Biskaborn, Boris K., Smith, S.L., Noetzli, J., Matthes, H., Vieira, G., Streletskiy, D.A., Schoeneich, P., Romanovsky, V.E., Lewkowicz, A.G., Abramov, A., Allard, M., Boike, J., Cable, W.L., Christiansen, H.H., Delaloye, R., Diekmann, B., Drozdov, D., Etzelmüller, B., Grosse, G., Lantuit, H., 2019. Permafrost is warming at a global scale. Nature Communications 10 (1), 264. https://doi.org/10.1038/s41467-018-08240-4.

Blok, D., Heijmans, M.M.P.D., Schaepman-Strub, G., Kononov, A.V., Maximov, T.C., Berendse, F., 2010. Shrub expansion may reduce summer permafrost thaw in Siberian tundra. Glob. Chang. Biol. 16 (4), 1296–1305. https://doi.org/10.1111/j.1365-2486.2009.02110.x.

Blunden, J., Arndt, D.S., 2019. State of the climate in 2018. Bull. Am. Meteorol. Soc. 100 (9), Si–S306. https://doi.org/10.1175/2019BAMSStateoftheClimate.1.

Bonan, G., 2015. Ecological Climatology: Concepts and Applications, 3rd ed. Cambridge University Press. https://doi.org/10.1017/CBO9781107339200.

Bonfils, C.J.W., Phillips, T.J., Lawrence, D.M., Cameron-Smith, P., Riley, W.J., Subin, Z. M., 2012. On the influence of shrub height and expansion on northern high latitude climate. Environ. Res. Lett. 7 (1), 015503 https://doi.org/10.1088/1748-9326/7/1/015503.

Bonnaventure, P.P., Lewkowicz, A.G., 2012. Permafrost probability modeling above and below treeline, Yukon, Canada. Cold Reg. Sci. Technol. 79–80, 92–106. https://doi.org/10.1016/j.coldregions.2012.03.004.

Bowman, A.W., Azzalini, A., 1997. Applied Smoothing Techniques for Data Analysis: The Kernel Approach with S-Plus Illustrations. OUP Oxford.

Brown, J., Sidlauskas, F.J., Delinski, G., 1997. Circum-Arctic Map of Permafrost and Ground Ice Conditions [Map]. The Survey. For sale by Information Services.

Bulygina, O.N., Razuvaev, V.N., 2012. Daily temperature and precipitation data for 518 Russian meteorological stations (1881—2010). In: Environmental System Science Data Infrastructure for a Virtual Ecosystem. Carbon Dioxide Information Analysis Center (CDIAC), Oak Ridge National Laboratory (ORNL), Oak Ridge, TN (United States). https://doi.org/10.3334/CDIAC/cli.100.

Chadburn, S.E., Burke, E.J., Cox, P.M., Friedlingstein, P., Hugelius, G., Westermann, S., 2017. An observation-based constraint on permafrost loss as a function of global warming. Nat. Clim. Chang. 7 (5), 340–344. https://doi.org/10.1038/nclimate3262.

Cheng, G., Wu, T., 2007. Responses of permafrost to climate change and their environmental significance, Qinghai-Tibet Plateau. J. Geophys. Res. Earth Surf. 112 (F2) https://doi.org/10.1029/2006JF000631.

Christiansen, H.H., Etzelmüller, B., Isaksen, K., Juliussen, H., Farbrot, H., Humlum, O., Johansson, M., Ingeman-Nielsen, T., Kristensen, L., Hjort, J., Holmlund, P., Sannel, A.B.K., Sigsgaard, C., Åkerman, H.J., Foged, N., Blikra, L.H., Pernosky, M.A., Ødegård, R.S., 2010. The thermal state of permafrost in the nordic area during the international polar year 2007–2009. Permafr. Periglac. Process. 21 (2), 156–181. https://doi.org/10.1002/ppp.687.

Côté, J., Konrad, J.-M., 2005a. Thermal conductivity of base-course materials. Can. Geotech. J. 42 (1), 61–78. https://doi.org/10.1139/t04-081.

Côté, J., Konrad, J.-M., 2005b. A generalized thermal conductivity model for soils and construction materials. Can. Geotech. J. 42 (2), 443–458. https://doi.org/10.1139/t04-106.

Davidson, E.A., Janssens, I.A., 2006. Temperature sensitivity of soil carbon decomposition and feedbacks to climate change. Nature 440 (7081), 165–173. https://doi.org/10.1038/nature04514.

Euskirchen, E.S., Mcquire, A.D., Chapin, F.S., 2007. Energy feedbacks of northern high-latitude ecosystems to the climate system due to reduced snow cover during 20th century warming. Glob. Chang. Biol. 13 (11), 2425–2438. https://doi.org/10.1111/j.1365-2486.2007.01450.x.

Fernández-Martínez, M., Sardans, J., Chevallier, F., Ciais, P., Obersteiner, M., Vicca, S., Canadell, J.G., Bastos, A., Friedlingstein, P., Sitch, S., Piao, S.L., Janssens, I.A., Peñuelas, J., 2019. Global trends in carbon sinks and their relationships with CO2 and temperature. Nat. Clim. Chang. 9 (1), 73–79. https://doi.org/10.1038/s41558-018-0367-7.

Fountain, A.G., Campbell, J.L., Schuur, E.A.G., Stammerjohn, S.E., Williams, M.W., Ducklow, H.W., 2012. The disappearing cryosphere: impacts and ecosystem responses to rapid cryosphereILoss. BioScience 62 (4), 405–415. https://doi.org/10.1525/bio.2012.62.4.11.

Gehan, E.A., 1965. A generalized Wilcoxon test for comparing arbitrarily singly-censored samples. Biometrika 52 (1–2), 203–224. https://doi.org/10.1093/biomet/52.1-2.203.

Gilichinsky, D.A., Barry, R.G., Bykhovets, S.S., Sorokovikov, V.A., Zhang, T., Zudin, S.L., Fedorov-Davydov, D.G., 1998. A century of temperature observation s of soil climate: Methods of analysis and long-term trends. In: Proceedings of 7th International Conference on Permafrost, pp. 313–317.

Groisman, P., Shugart, H., Kicklighter, D., Henebry, G., Tchebakova, N., Maksyutov, S., Monier, E., Gutman, G., Gulev, S., Qi, J., Prishchepov, A., Kukavskaya, E., Porfiriev, B., Shiklomanov, A., Loboda, T., Shiklomanov, N., Nghiem, S., Bergen, K., Albrechtová, J., Zolina, O., 2017. Northern Eurasia Future Initiative (NEFI): Facing the challenges and pathways of global change in the twenty-first century. Prog. Earth Planet. Sci. 4 (1), 41. https://doi.org/10.1186/s40645-017-0154-5.

Grosse, G., Goetz, S., McGuire, A.D., Romanovsky, V.E., Schuur, E.A.G., 2016. Changing permafrost in a warming world and feedbacks to the Earth system. Environ. Res. Lett. 11 (4), 040201 https://doi.org/10.1088/1748-9326/11/4/040201.

Gruber, S., 2012. Derivation and analysis of a high-resolution estimate of global permafrost zonation. Cryosphere 6 (1), 221–233. https://doi.org/10.5194/tc-6-221-2012.

Guo, D., Wang, H., 2016. CMIP5 permafrost degradation projection: A comparison among different regions. J. Geophys. Res. Atmos. 121 (9), 4499–4517. https://doi.org/10.1002/2015JD024108.

Heimann, M., Reichstein, M., 2008. Terrestrial ecosystem carbon dynamics and climate feedbacks. Nature 451 (7176), 289–292. https://doi.org/10.1038/nature06591.

Hijmans, R.J., Cameron, S.E., Parra, J.L., Jones, P.G., Jarvis, A., 2005. Very high resolution interpolated climate surfaces for global land areas. Int. J. Climatol. 25 (15), 1965–1978. https://doi.org/10.1002/joc.1276.

Hinkel, K.M., 1997. Estimating seasonal values of thermal diffusivity in thawed and frozen soils using temperature time series. Cold Reg. Sci. Technol. 26 (1), 1–15. https://doi.org/10.1016/S0165-232X(97)00004-9.

Hirota, T., Pomeroy, J.W., Granger, R.J., Maule, C.P., 2002. An extension of the force-restore method to estimating soil temperature at depth and evaluation for frozen soils under snow. J. Geophys. Res. Atmos. 107 (D24) https://doi.org/10.1029/2001JD001280. ACL 11-1-ACL 11–10.

Hjort, J., Karjalainen, O., Aalto, J., Westermann, S., Romanovsky, V.E., Nelson, F.E., Etzelmüller, B., Luoto, M., 2018. Degrading permafrost puts Arctic infrastructure at risk by mid-century. Nat. Commun. 9 (1), 5147. https://doi.org/10.1038/s41467-018-07557-4.

Iijima, Y., Fedorov, A.N., Park, H., Suzuki, K., Yabuki, H., Maximov, T.C., Ohata, T., 2010. Abrupt increases in soil temperatures following increased precipitation in a permafrost region, Central Lena River basin, Russia. Permafr. Periglac. Process. 21 (1), 30–41. https://doi.org/10.1002/ppp.662.

Jacobs, A.F.G., Heusinkveld, B.G., Holtslag, A.A.M., 2011. Long-term record and analysis of soil temperatures and soil heat fluxes in a grassland area, the Netherlands. Agric. For. Meteorol. 151 (7), 774–780. https://doi.org/10.1016/j.agrformet.2011.01.002.

Jafarov, E.E., Coon, E.T., Harp, D.R., Wilson, C.J., Painter, S.L., Atchley, A.L., Romanovsky, V.E., 2018. Modeling the role of preferential snow accumulation in through talik development and hillslope groundwater flow in a transitional permafrost landscape. Environ. Res. Lett. 13 (10), 105006. https://doi.org/10.1088/1748-9326/aadd30.

James, M., Lewkowicz, A.G., Smith, S.L., Miceli, C.M., 2013. Multi-decadal degradation and persistence of permafrost in the Alaska Highway corridor, Northwest Canada. Environ. Res. Lett. 8 (4), 045013 https://doi.org/10.1088/1748-9326/8/4/045013.

Jobbágy, E.G., Jackson, R.B., 2000. The vertical distribution of soil organic carbon and its relation to climate and Vegetation. Ecol. Appl. 10 (2), 423–436. https://doi.org/10.1890/1051-0761(2000)010[0423:TVDOSO]2.0.CO;2.

Jones, A., Stolbovay, V., Tarnocai, C., Broll, G., Spaargaren, O., Montanarella, L., 2010. Soil Atlas of the Northern Circumpolar Region. Soil Atlas of the Northern Circumpolar Region. https://www.cabdirect.org/cabdirect/abstract/20103342230.

Jorgenson, M.T., Romanovsky, V., Harden, J., Shur, Y., O'Donnell, J., Schuur, E.A.G., Kanevskiy, M., Marchenko, S., 2010. Resilience and vulnerability of permafrost to climate changeThis article is one of a selection of papers from the Dynamics of Change in Alaska's Boreal Forests: Resilience and Vulnerability in Response to climate Warming. Can. J. For. Res. 40 (7), 1219–1236. https://doi.org/10.1139/X10-060.

Karjalainen, O., Luoto, M., Aalto, J., Hjort, J., 2019. New insights into the environmental factors controlling the ground thermal regime across the Northern Hemisphere: a comparison between permafrost and non-permafrost areas. Cryosphere 13 (2), 693–707. https://doi.org/10.5194/tc-13-693-2019.

Lawrence, D.M., Slater, A.G., 2010. The contribution of snow condition trends to future ground climate. Clim. Dyn. 34 (7–8), 969–981. https://doi.org/10.1007/s00382-009-0537-4.

Lugina, K.M., Groisman, P.Y., Vinnikov, K.Y., Koknaeva, V.V., Speranskaya, N.A., 2006. Monthly surface air temperature time series area-averaged over the 30-degree latitudinal belts of the globe, 1881-2005. In: In Trends: A Compendium of Data on Global Change. Carbon Dioxide Information Analysis Center, Oak Ridge National Laboratory, U.S. Department of Energy, Oak Ridge, Tenn., U.S.A. https://doi.org/10.3334/CDIAC/cli.003.

MacDougall, A.H., Avis, C.A., Weaver, A.J., 2012. Significant contribution to climate warming from the permafrost carbon feedback. Nat. Geosci. 5 (10), 719–721. https://doi.org/10.1038/ngeo1573.

Morse, P.D., Burn, C.R., Kokelj, S.V., 2012. Influence of snow on near-surface ground temperatures in upland and alluvial environments of the outer Mackenzie Delta, Northwest Territories [1] this article is one of a series of papers published in this CJES special issue on the theme of Fundamental and applied research on permafrost in Canada. Can. J. Earth Sci. 49 (8), 895–913. https://doi.org/10.1139/e2012-012.

Nauta, A.L., Heijmans, M.M.P.D., Blok, D., Limpens, J., Elberling, B., Gallagher, A., Li, B., Petrov, R.E., Maximov, T.C., van Huissteden, J., Berendse, F., 2015. Permafrost collapse after shrub removal shifts tundra ecosystem to a methane source. Nat. Clim. Chang. 5 (1), 67–70. https://doi.org/10.1038/nclimate2446.

Palmer, M.J., Burn, C.R., Kokelj, S.V., 2012. Factors influencing permafrost temperatures across tree line in the uplands east of the Mackenzie Delta, 2004-2010. Can. J. Earth Sci. 49 (8), 877–894. https://doi.org/10.1139/e2012-002.

Park, H., Sherstiukov, A.B., Fedorov, A.N., Polyakov, I.V., Walsh, J.E., 2014. An observation-based assessment of the influences of air temperature and snow depth on soil temperature in Russia. Environ. Res. Lett. 9 (6), 064026 https://doi.org/10.1088/1748-9326/9/6/064026.

Pavlov, A.V., 1994. Current changes of climate and permafrost in the arctic and sub-arctic of Russia. Permafr. Periglac. Process. 5 (2), 101–110. https://doi.org/10.1002/ppp.3430050204.

Phillips, C.L., 2020. How much will soil warm? J. Geophys. Res. Biogeosci. https://doi.org/10.1029/2020JG005668.

Porter, J.R., Gawith, M., 1999. Temperatures and the growth and development of wheat: a review. Eur. J. Agron. 10 (1), 23–36. https://doi.org/10.1016/S1161-0301(98)00047-1.

Qian, B., Gregorich, E.G., Gameda, S., Hopkins, D.W., Wang, X.L., 2011. Observed soil temperature trends associated with climate change in Canada. J. Geophys. Res. Atmos. 116 (D2) https://doi.org/10.1029/2010JD015012.

R Core Team, 2017. R: A Language and Environment for Statistical Computing. R Foundation for Statistical Computing, Vienna, Austria. https://www.r-project.org/.

Romanovsky, V.E., Sazonova, T.S., Balobaev, V.T., Shender, N.I., Sergueev, D.O., 2007. Past and recent changes in air and permafrost temperatures in eastern Siberia. Glob. Planet. Chang. 56 (3), 399–413. https://doi.org/10.1016/j.gloplacha.2006.07.022.

Romanovsky, Vladimir E., Smith, S.L., Christiansen, H.H., 2010. Permafrost thermal state in the polar Northern Hemisphere during the international polar year 2007–2009: a synthesis. Permafr. Periglac. Process. 21 (2), 106–116. https://doi.org/10.1002/ppp.689.

Romanovsky, V.E., Smith, S.L., Christiansen, H.H., Shiklomanov, N.I., Streletskiy, D.A., Drozdov, D.S., Malkova, G.V., Oberman, N.g., Kholodov, A.L., Marchenko, S.S., 2019. Terrestrial permafrost [in "State of the Climate in 2018"]. Bull. Amer. Meteor. Soc. 100 (9), S153–S156. https://doi.org/10.1175/2019BAMSStateoftheClimate.1.

Schuur, E.A.G., Abbott, B.W., Bowden, W.B., Brovkin, V., Camill, P., Canadell, J.G., Chanton, J.P., Chapin, F.S., Christensen, T.R., Ciais, P., Crosby, B.T., Czimczik, C.I., Grosse, G., Harden, J., Hayes, D.J., Hugelius, G., Jastrow, J.D., Jones, J.B., Kleinen, T., Zimov, S.A., 2013. Expert assessment of vulnerability of permafrost carbon to climate change. Climatic Change 119 (2), 359–374. https://doi.org/10.1007/s10584-013-0730-7.

Schuur, E.a.G., McGuire, A.D., Schädel, C., Grosse, G., Harden, J.W., Hayes, D.J., Hugelius, G., Koven, C.D., Kuhry, P., Lawrence, D.M., Natali, S.M., Olefeldt, D., Romanovsky, V.E., Schaefer, K., Turetsky, M.R., Treat, C.C., Vonk, J.E., 2015. Climate change and the permafrost carbon feedback. Nature 520 (7546), 171–179. https://doi.org/10.1038/nature14338.

Serreze, M.C., Barrett, A.P., Stroeve, J.C., Kindig, D.N., Holland, M.M., 2009. The emergence of surface-based Arctic amplification. Cryosphere 3 (1), 11–19. https://doi.org/10.5194/tc-3-11-2009.

Sherstiukov, A., 2012. СТАТИСТИЧЕСКИЙ КОНТРОЛЬ МАССИВА СУТОЧНЫХ ДАННЫХ ТЕМПЕРАТУРЫ ПОЧВОГРУНТОВ (statistical quality control of Soil Temperature Dataset). no. 176, pp. 224–232. http://meteo.ru/index.php?option=com_docman&task=doc_download&gid=107.

Smith, S.L., Romanovsky, V.E., Lewkowicz, A.G., Burn, C.R., Allard, M., Clow, G.D., Yoshikawa, K., Throop, J., 2010. Thermal state of permafrost in North America: a contribution to the international polar year. Permafr. Periglac. Process. 21 (2), 117–135. https://doi.org/10.1002/ppp.690.

Smith, S.L., Throop, J., Lewkowicz, A.G., Burn, C.R., 2012. Recent changes in climate and permafrost temperatures at forested and polar desert sites in northern Canada. Canadian Journal of Earth Sciences 49 (8), 914–924. https://doi.org/10.1139/e2012-019.

Smith, Sharon L., Riseborough, D.W., Bonnaventure, P.P., Duchesne, C., 2016. An ecoregional assessment of freezing season air and ground surface temperature in the Mackenzie Valley corridor, NWT, Canada. Cold Reg. Sci. Technol. 125, 152–161. https://doi.org/10.1016/j.coldregions.2016.02.007.

Stieglitz, M., Déry, S.J., Romanovsky, V.E., Osterkamp, T.E., 2003. The role of snow cover in the warming of arctic permafrost. Geophys. Res. Lett. 30 (13) https://doi.org/10.1029/2003GL017337.

Streletskiy, D.A., Biskaborn, B.K., Noetz, J., Romanovsky, V.E., 2017. Permafrost thermal state. Bull. Am. Meteorol. Soc. 98 (8), 19–21. https://doi.org/10.1175/2017BAMSStateoftheClimate.1.

Tarnocai, C., Canadell, J.G., Schuur, E. a. G., Kuhry, P., Mazhitova, G., & Zimov, S., 2009. Soil organic carbon pools in the northern circumpolar permafrost region. Glob. Biogeochem. Cycles 23 (2). https://doi.org/10.1029/2008GB003327.

Taylor, A.E., Wang, K., Smith, S.L., Burgess, M.M., Judge, A.S., 2006. Canadian Arctic permafrost observatories: detecting contemporary climate change through inversion of subsurface temperature time series. J. Geophys. Res. Solid Earth 111 (B2). https://doi.org/10.1029/2004JB003208.

Tchebakova, N.M., Rehfeldt, G.E., Parfenova, E.I., 2010. From vegetation zones to climatypes: Effects of climate warming on siberian ecosystems. In: Osawa, A., Zyryanova, O.A., Matsuura, Y., Kajimoto, T., Wein, R.W. (Eds.), Permafrost Ecosystems: Siberian Larch Forests. Springer Netherlands, pp. 427–446. https://doi.org/10.1007/978-1-4020-9693-8_22.

Throop, J., Lewkowicz, A.G., Smith, S.L., 2012. Climate and ground temperature relations at sites across the continuous and discontinuous permafrost zones, northern Canada. Can. J. Earth Sci. 49 (8), 865–876. https://doi.org/10.1139/e11-075.

Tingjun, Z., 2005. Influence of the seasonal snow cover on the ground thermal regime: an overview. Rev. Geophys. 43 (4) https://doi.org/10.1029/2004RG000157.

Turetsky, M.R., Abbott, B.W., Jones, M.C., Anthony, K.W., Olefeldt, D., Schuur, E.A.G., Grosse, G., Kuhry, P., Hugelius, G., Koven, C., Lawrence, D.M., Gibson, C., Sannel, A. B.K., McGuire, A.D., 2020. Carbon release through abrupt permafrost thaw. Nat. Geosci. 13 (2), 138–143. https://doi.org/10.1038/s41561-019-0526-0.

Vardon, P.J., 2015. Climatic influence on geotechnical infrastructure: a review. Environ. Geotech. 2 (3), 166–174. https://doi.org/10.1680/envgeo.13.00055.

Vieira, G., Bockheim, J., Guglielmin, M., Balks, M., Abramov, A.A., Boelhouwers, J., Cannone, N., Ganzert, L., Gilichinsky, D.A., Goryachkin, S., López-Martínez, J., Meiklejohn, I., Raffi, R., Ramos, M., Schaefer, C., Serrano, E., Simas, F., Sletten, R., Wagner, D., 2010. Thermal state of permafrost and active-layer monitoring in the antarctic: advances during the international polar year 2007–2009. Permafr. Periglac. Process. 21 (2), 182–197. https://doi.org/10.1002/ppp.685.

Walker, D.A., Jia, G.J., Epstein, H.E., Raynolds, M.K., Iii, F.S.C., Copass, C., Hinzman, L. D., Knudson, J.A., Maier, H.A., Michaelson, G.J., Nelson, F., Ping, C.L., Romanovsky, V.E., Shiklomanov, N., 2003. Vegetation-soil-thaw-depth relationships along a low-arctic bioclimate gradient, Alaska: synthesis of information from the ATLAS studies. Permafr. Periglac. Process. 14 (2), 103–123. https://doi.org/10.1002/ppp.452.

Walker, D.A., Raynolds, M.K., Daniëls, F.J.A., Einarsson, E., Elvebakk, A., Gould, W.A., Katenin, A.E., Kholod, S.S., Markon, C.J., Melnikov, E.S., Moskalenko, N.G., Talbot, S.S., Yurtsev, B.A., Team, T. other members of the C, 2005. The circumpolar arctic vegetation map. J. Veg. Sci. 16 (3), 267–282. https://doi.org/10.1111/j.1654-1103.2005.tb02365.x.

Walvoord, M.A., Kurylyk, B.L., 2016. Hydrologic impacts of thawing permafrost—A review. Vadose Zone J. 15 (6) https://doi.org/10.2136/vzj2016.01.0010.

Westermann, S., Boike, J., Langer, M., Schuler, T.V., Etzelmüller, B., 2011. Modeling the impact of wintertime rain events on the thermal regime of permafrost. Cryosphere 5 (4), 945–959. https://doi.org/10.5194/tc-5-945-2011.

Wickham, H., 2016. ggplot2: Elegant Graphics for Data Analysis. Springer-Verlag. https://www.springer.com/gp/book/9780387981413.

Yi, S., Woo, M., Arain, M.A., 2007. Impacts of peat and vegetation on permafrost degradation under climate warming. Geophys. Res. Lett. 34 (16) https://doi.org/10.1029/2007GL030550.

Zhang, T., Barry, R.G., Gilichinsky, D., Bykhovets, S.S., Sorokovikov, V.A., Ye, J., 2001. An amplified signal of climatic change in soil temperatures during the last century at Irkutsk, Russia. Clim. Chang. 49 (1), 41–76. https://doi.org/10.1023/A:1010790203146.

Zhang, Y., Sherstiukov, A.B., Qian, B., Kokelj, S.V., Lantz, T.C., 2018. Impacts of snow on soil temperature observed across the circumpolar north. Environ. Res. Lett. 13 (4), 044012 https://doi.org/10.1088/1748-9326/aab1e7.

Zhao, L., Wu, Q., Marchenko, S.S., Sharkhuu, N., 2010. Thermal state of permafrost and active layer in Central Asia during the international polar year. Permafr. Periglac. Process. 21 (2), 198–207. https://doi.org/10.1002/ppp.688.